NASA TECHNICAL MEMORANDUM

NASA TM X-1110

NASA TM X-1110

FACILITY FORM 602

N65-29953 (ACCESSION NUMBER) (THRU)

30 (PAGES) 1 (CODE)

(NASA CR OR TMX OR AD NUMBER) 01 (CATEGORY)

GPO PRICE $

CFSTI PRICE(S) $

Hard copy (HC)

Microfiche (MF)

ff 653 July 65

USE OF A SINGLE TURNING VANE TO ELIMINATE FLOW SEPARATION IN A SPACE-LIMITED 90° INTAKE ELBOW OF AN AXIAL-FLOW COMPRESSOR

by S. Z. Pinckney

Langley Research Center

Langley Station, Hampton, Va.

NATIONAL AERONAUTICS AND SPACE ADMINISTRATION • WASHINGTON, D. C. • AUGUST 1965

NASA TM X-1110

USE OF A SINGLE TURNING VANE TO ELIMINATE FLOW SEPARATION IN A SPACE-LIMITED 90° INTAKE ELBOW OF AN AXIAL-FLOW COMPRESSOR

By S. Z. Pinckney

Langley Research Center
Langley Station, Hampton, Va.

NATIONAL AERONAUTICS AND SPACE ADMINISTRATION

For sale by the Clearinghouse for Federal Scientific and Technical Information
Springfield, Virginia 22151 – Price $2.00

USE OF A SINGLE TURNING VANE TO ELIMINATE FLOW SEPARATION IN A SPACE-LIMITED 90° INTAKE ELBOW OF AN AXIAL-FLOW COMPRESSOR

By S. Z. Pinckney
Langley Research Center

29953

SUMMARY

The performance of a 90° inlet elbow of an axial-flow compressor was determined for the purpose of improving the elbow exit-flow distribution. The flow passage through the elbow changed from circular at the inlet to annular at the exit because a rotor-bearing housing was located in the center of the elbow. The elbow design was severely limited relative to optimum proportions. Exit total-pressure surveys of the original elbow design revealed regions of low velocity on the inner part of the elbow. The addition of a single vane greatly reduced the extent of low-energy regions.

Author

INTRODUCTION

Elbows which sharply turn ducted airflow are in general use in various types of industrial equipment as well as in aircraft. These elbows are frequently designed within such space limitations that optimum proportions cannot be used. These deficiencies result in high total-pressure losses and nonuniform velocity distributions at the elbow exit, particularly downstream of the inner part of the turn where separation frequently occurs (ref. 1). It is well known that nonuniform elbow exit-flow distributions can cause premature stall of the compressor and local hot spots in the flow after compression.

Various methods have been reported for improving the performance of elbows designed with space limitations; the use of rows of turning vanes (ref. 2) and the use of vortex generators (ref. 3) are examples. Reference 2 reveals that rows of turning vanes help the airflow negotiate the turn, and reference 3 reveals that vortex generators help to eliminate flow separation on the inside of the turn.

The present investigation is of a 90° intake elbow upstream of a multistage, axial-flow compressor. The severe space limitations under which the elbow was designed created an extremely small inner-turn radius which is the origin of a large separated flow region at the exit of the elbow. A comparison of this design with an optimum design as determined from reference 1 is shown in figure 1. The present investigation revealed that separation regions of the

type originating at the inner part of the turn can be eliminated by the addition of a single turning vane upstream of and near the inner turn. Total-pressure and velocity surveys of the inlet elbow with and without the added vane are presented.

SYMBOLS

D	inlet diameter
p_t	total pressure
p	static pressure
q	dynamic pressure, $\frac{\rho V^2}{2}$
V	velocity
ρ	mass density
β	flow angle measured from axis of rotation of rotor hub
$\frac{\Delta p_t}{(p_t - p)_i}$	loss coefficient, $\frac{(p_{t,i} - p_{t,e})}{(p_t - p)_i}$

Subscripts:

i	elbow inlet reference station as indicated in figure 2(a)
e	elbow exit
1	elbow survey station as shown in figure 2(a) or 2(d)
2	elbow survey station as shown in figure 2(a)

APPARATUS

Inlet Elbow

Figure 2(a) is a diagram showing the experimental setup as well as the physical relationship of the various parts of the inlet elbow. The inlet duct is circular and is followed by a transition region which transforms the circular ducting into a rectangle. Extending from the rear wall of the elbow and out through the elbow exit are the rotor-bearing housing and a simulated rotor hub that result in an annular area at the exit of the elbow. In order better to

simulate actual operating conditions at the exit, a stator-blade housing was installed around the rotor-bearing housing and simulated rotor hub.

The outer half of the flow entering the elbow has to pass around the rotor-bearing housing while the inner half has to make a sharp turn of which the inner radius is only 0.083 inlet diameter. A splitter plate (fig. 2(b)) was located on the inlet side of the rotor-bearing housing. Figure 2(b) shows a set of concentric circular vanes that help to turn the flow around the rotor-bearing housing onto a deflection plate. The deflection plate then turns the flow into a row of vanes (vane detail, fig. 2(b)), which turn the flow out the exit of the elbow. Upon passing through these turning vanes and out the elbow exit, the flow enters the annulus formed by the stator-blade housing and the simulated rotor hub. At this point the flow passes through a set of guide vanes (fig. 2(a)) having NACA 65-series compressor blade sections as described in references 4 and 5. These guide vanes were set at an angle of attack of 24° at the blade root. After passing through the annulus formed by the stator-blade housing and simulated rotor hub, the flow is then exhausted to atmosphere.

A single turning vane which has the same shape and radius as existing vanes was designed and installed in the elbow as a vane modification. This vane was movable during tests conducted to optimize its location and was placed close to the inner wall of the elbow. (Fig. 2(c) shows the final position.) In the final position of the single vane, the center of the vane chord was slightly upstream of the center of turn of the inner wall. The chord and leading edge were, respectively, at angles of 30° and $2\frac{1}{2}^\circ$ with respect to the inlet flow; the incoming flow was turned through an angle of $57\frac{1}{2}^\circ$; the contraction ratio between vane and elbow inner wall was approximately 2:1. The single vane had a semispan of 0.259 inlet diameter with a supporting plate from the vane tip to the elbow inner wall. In order to eliminate excessive flow blockage, vane 1 and the leading 16.1° of vane 2 (fig. 2(c)) were removed for the final elbow vane modification. The inner wall of the elbow exit was faired into the exit duct to eliminate the sudden expansion which results in separation of the flow (fig. 2(c)).

The air was furnished by a centrifugal compressor which had a flow capacity of 80 000 cubic feet per minute and a pressure rise of 1/8 atmosphere. The airflow was taken into the compressor from the atmosphere and pumped into a settling chamber from which a duct passed to the elbow inlet. The airflow was delivered to the inlet reference station at a Mach number of approximately 0.08 and Reynolds number per foot of approximately 6.8×10^5. The flow through the elbow was discharged into the atmosphere at the elbow exit.

Instrumentation

Four equispaced wall static-pressure orifices and a reference total-pressure tube were located at the inlet reference station of the elbow (fig. 2(a)). Exit total pressures and flow-angle measurements were made at two elbow exit stations, 1 and 2, as indicated in figure 2(a). The inlet reference-station wall static pressures and the exit total-pressure surveys

were measured by differential-pressure transducers and recorded on electronic data recorders for which the total pressure at the inlet reference station was used as a reference. A set of circumferential static-pressure orifices were installed on the rotor hub downstream of its rotatable section and values were read on mercury manometers.

Exit-flow direction and total pressures were measured by means of a combination total-pressure and flow-direction probe of the prism type with the yaw surface inclined 45° to the direction normal to the flow. Details of this probe are described in reference 6. An automatic null device that was used consisted of a pressure switch which changed the direction of a direct-current motor and thus the direction of the survey probe. The null device hunted ±1° about the mean; the flow angles are believed to be accurate to approximately ±1°. Overall system accuracy for pressure measurements is on the order of ±1 percent or less.

PROCEDURE

The inlet-flow investigation of the elbow consisted of total-pressure surveys and wall static-pressure measurements made at the inlet reference station of the inlet elbow (fig. 2(a)). The inlet total-pressure surveys were conducted perpendicular to the duct wall at several stations around the duct.

A part of the exit-flow investigation of the elbow was conducted without the stator-blade housing and simulated rotor hub (fig. 2(d)) at the exit of the elbow. A second part of the exit-flow investigation was conducted with a stator-blade housing and simulated rotor hub (fig. 2(a)) and with and without the original vane configuration. Tests were conducted with and without guide vanes for both the original and the modified vane configurations. This test program is outlined as follows:

(1) Without a stator-blade housing or simulated rotor hub (exit station 1)

(2) With a stator-blade housing, simulated rotor hub, and the original vane configuration (exit station 2)
  (a) Without guide vanes
  (b) With guide vanes

(3) With a stator-blade housing, simulated rotor hub, and the modified vane configuration (exit station 2)
  (a) Without guide vanes
  (b) With guide vanes

With the stator-blade housing removed, total-pressure and flow-direction surveys were conducted at exit station 1. (See fig. 2(a).) The location of the survey points is shown in figure 2(d) (x-1 through x-9 and y-1 through y-7). All surveys were initiated at the outer wall and were either parallel with or perpendicular to the vane passages.

With the stator-blade housing installed, total-pressure and flow-direction surveys were made and static-pressure measurements were taken in the region of

the first row of rotor blades (exit survey station 2). (See fig. 2(a).) These surveys were conducted by setting the survey probe at a known radial distance from the rotor hub and then revolving the rotor hub and probe as a unit. In this manner, continuous circumferential surveys were obtained at several radial positions. The shank of the survey probe was inclined 5° from the normal to the rotor-hub surface in order to minimize errors in pressure measurements in the region near the stator-blade housing, as well as to maintain a nearly constant distance between the probe and the trailing edge of the guide vanes, which were tapered from rotor hub to stator shell. Eight surveys with and without guide vanes were considered sufficient. The eight surveys without the guide vanes covered 180° of circumferential angle, whereas those with the guide vanes covered 360° of circumferential angle. Figure 2(a) shows the relative positions of circumferential angles.

Tests with the stator-blade housing were repeated in the same general manner when the vane modifications were made. The surveys without guide vanes, however, were made only at circumferential angles from 90° to 180° (fig. 2(a)); whereas those with the guide vanes, as before, were made at circumferential angles from 0° to 360°. The angle of attack of the movable vane was varied from 0° to 35°. The distance of the midchord of the single added vane from the elbow inner wall was varied from the position shown in figure 2(c) toward the slanted back wall. The vane semispan, as measured from the surface of the elbow-inlet splitter plate to the vane tip, was varied from 0.259 to 0.333 inlet diameter.

RESULTS AND DISCUSSION

Inlet-Flow Distribution

Representation of the inlet flow in terms of distributions of dynamic pressure $(p_t - p)_i$ revealed a uniform flow entering the elbow. The reference total pressure in the inlet of the elbow is located in the uniform-flow region external to the boundary layer.

Performance With No Stator-Blade Housing or Rotor Hub

The results from the surveys made at exit station 1 of the elbow without a stator-blade housing or rotor hub are presented in figure 3. The experimental data are presented in the form of models of the pressure contours at the various x- and y-stations shown in figure 2(d), because representation by this means was believed to allow a better general grasp of the flow conditions at the elbow exit. Photographs of these contour models were taken from several angles (identified arbitrarily as views A to E) in the interest of providing a clearer view of the contours. The height of the contours in the photographs represents $(p_t - p)_{e,1}$, or exit q. The static pressure p in the $(p_t - p)_{e,1}$ contours is assumed to be atmospheric pressure. In figure 3 the difference between the height of the plastic shells and the contours is equal to Δp_t, the

total-pressure loss through the elbow. The local flow directions are represented by the arrows drawn on the $(p_t - p)_{e,1}$ contours.

Figures 3(a) and 3(d) show no flow where profile (x-1) is located, that is, in the midregion between the first vane and the inner wall surface. As can be seen from profile (y-1) (figs. 3(b) and 3(e)), only a small region of low-velocity flow in the vicinity of vane 1 is indicated in the vane passage of profile (x-1); whereas no flow is indicated in the remainder of this region. The vane passage of profile (x-2) (figs. 3(a) and 3(e)) has no flow in the neighborhood of the circular innerbody and the horizontal support plate (labeled ℄ in fig. 2(d)) but has a high flow rate with relatively little total-pressure loss in the major portion of the passage. Tuft studies of the vane passages of profiles (x-1) and (x-2) indicated radical flow oscillations which are indicative of flow separation.

The total-pressure loss or velocity deficiency in the region of profiles (x-8) and (x-9) (figs. 3(a) and 3(e)) is caused by the wake of the circular vane and separated regions adjacent to it. The origins of the separated-flow regions were determined by tuft studies to be the intersections of the back wall of the elbow with the circular vane and the back wall of the elbow with the rotor-bearing housing (fig. 2(d)). These separated-flow regions resulted in two vortices at the exit plane. The wake of the splitter vane is quite evident throughout the rear half of the elbow exit.

Measurements of the flow angle showed that vane underturning of the flow (shown by arrows in the y-contours of figs. 3(b) and 3(c)) on the order of 15° was not uncommon, and underturning to 30° was quite evident at the rear of the elbow exit. In addition to the general underturning characteristics of the elbow, the flow (x-surveys of fig. 3(a)) was away from the center line in the front half of the exit and toward the center line in the rear half of the exit. Frequently, these flow angles relative to the center line were on the order of 30°. The large total-pressure losses, severe velocity gradients, and excessive exit-flow-angle diversions indicate the inadequacy of the vane design of the elbow.

Performance With Stator-Blade Housing, Simulated Rotor Hub, and Original Vane Configuration

Without guide vanes.- For various circumferential locations (fig. 2(a)), the radial variation of loss coefficient $\frac{\Delta p_t}{(p_t - p)_i}$ is shown for survey station 2 in figure 4. These data indicate that regions adjacent to the rotor hub and stator walls corresponded to a total-pressure loss Δp_t equal to the inlet $(p_t - p)_i$ over a circumferential distance extending from circumferential angles of 90° to 140°. If the elbow exit flow is assumed to be symmetrical, this same deficiency also extended from circumferential angles of 220° to 270°. In addition, a region downstream from the inner part of the elbow (circumferential

angle of 175°) indicated a loss of about three times the inlet $(p_t - p)_i$. Static-pressure surveys, which are not shown herein, revealed a maximum circumferential variation of approximately twice the inlet $(p_t - p)_i$. Observation of surveys of the direction of flow angle, which is defined as clockwise or counterclockwise by an observer looking downstream, showed considerable variation, especially in the region near the rotor hub. For a survey at the 0.054 passage-width station, the flow at a circumferential angle of 20° was 30° in a counterclockwise direction, whereas the flow at a circumferential angle of 130° was 26° in a clockwise direction. At a circumferential angle of 10° a strong vortex existed with flow at 22° in a counterclockwise direction near the rotor hub and at angles in excess of 22° in a clockwise direction near the stator housing.

Velocity distributions corresponding to the loss-coefficient distribution of figure 4 are presented in figure 5 as a ratio,

$$\frac{V_{e,2}}{V_i} = \left[\frac{(p_t - p)_{e,2}}{(p_t - p)_i}\right]^{1/2}$$

The nondimensional velocity distributions of figure 5 are not immediately identifiable with the distributions of total-pressure loss coefficient of figure 4 because of the large circumferential static-pressure gradient. For instance, because of the low static pressure on the inner part of the turn for a circumferential angle of 175°, the velocity ratios are higher than might have been anticipated. This effect of static-pressure gradient is also evident in the regions near the rotor hub and stator walls at a circumferential angle of 140°. For comparison purposes, the velocity ratio obtained by the simple area-ratio relationship $\frac{A_i}{A_{e,2}}$ is, as indicated in the figure, about 1.5. Within the range of the data shown in figure 5, the variation in velocity ratio is from +25 percent to -50 percent of the calculated velocity ratio of 1.5.

With guide vanes.- The nondimensional velocity distributions obtained with the guide vanes installed are presented in figure 6. With the guide vanes installed, a low-energy region still existed in the region downstream from the inner part of the elbow (180° location). The static-pressure variation, not shown, was reduced in magnitude from that obtained without the guide vanes installed, and indicated a variation approximately equal to $(p_t - p)_i$. It is difficult to generalize as to which locations are free from turning-vane wakes because of the large number of wakes added by the guide vanes. Although the circumferential-angle location of 0° is relatively free of wakes and the circumferential-angle location of 175° is immersed in a low-energy region, the addition of the guide vanes, in general, made the flow more uniform, especially in the region of the annulus between the stations at 0.20 and 0.70 passage width. However, reference to the total-pressure distribution measurements (not shown) from which the velocity distributions of figure 6 were obtained showed that the addition of the guide vanes increased circumferentially the region of the low-energy flow of the inner part of the inlet elbow. The lower set of curves of

figure 6 show the asymmetry of flow when they are compared with curves for the opposite half, upper set of curves, of the annulus at the appropriate locations. A curve for the approximate average velocity ratio based on the area-ratio relationship $\frac{A_i}{A_{e,2}}\left(\frac{1}{\cos \beta}\right)$ lies below most of the velocity-ratio curves with the exception of that for a circumferential angle of 175°, where β represents the value of flow angle of the guide vanes predicted by references 4 and 5. With the addition of the guide vanes the variation in velocity ratio is reduced to from +23 percent to -35 percent of predicted values as compared with from +25 percent to -50 percent for the configuration without the guide vanes.

Flow-angle cross plots corresponding to the velocity profiles of figure 6 are presented in figure 7 for the elbow with guide vanes installed. These results show that, in general, the flow angularity varies in a manner similar to that predicted by the methods of references 4 and 5. An appreciable number of the points of figure 7 correspond to locations containing wakes or high-velocity gradients, or both, where the flow-angle measurement is not very accurate. The points at the 0.301-passage-width station correspond to a minimum of guide-vane wakes and velocity gradients and have the closest grouping. In general, the flow angle appears to be about 1° to 5° below the predicted values.

The addition of the guide vanes appears to produce a more uniform elbow exit velocity distribution and to eliminate the underturning effect of the elbow. Also, in general, the addition of the guide vanes increased circumferentially the region of low-energy flow of the inner part of the inlet elbow.

Performance With Stator-Blade Housing, Simulated Rotor Hub, and Modified Vane Configuration

The data presentations in the preceding sections indicated that vane 1 and possibly vane 2 (see fig. 2(c)) were ineffective. Therefore, the changes shown in figure 2(c) were made. Vane 1 and the leading 16.1° of vane 2 were removed (as indicated by dotted lines). The wooden fairing was added to eliminate the discontinuity in the duct; the final position, angle of attack, and span of the added vane represent nearly optimum values determined experimentally.

Without guide vanes.- A plot of the variation in loss coefficient for survey station 2 as a function of the radial distance from the rotor hub is shown in figure 8. The values for the original vane configuration from figure 4 are included for comparison. At the circumferential angle of 175° the reduction of loss coefficient from an average of about 2.7 (original vane configuration) to an average of about 0.8 was a direct result of the modified vane configuration. The changes in loss coefficient indicated for other circumferential angles were caused by small shifts in vane wakes and therefore are not realistic.

The velocity distributions corresponding to the total-pressure loss-coefficient distributions of figure 8 along with the original velocity distributions of figure 5 are presented in figure 9. The modified vane configuration produced an increase in velocity at all points on the surveys of circumferential angles

89° and 175°; however, reference to the continuous circumferential surveys from which figures 8 and 9 were obtained revealed the improvement at the 89° position was due to a wake shift. Where the range of data (shown in fig. 9) for the original vane configuration is from +25 percent to -50 percent of the average velocity ratio 1.5, the range of the data for the modified vane configuration is shown to be only from +25 percent to -20 percent. Figures 8 and 9 therefore show a considerable improvement in elbow exit-flow distribution with the modified vane configuration.

With guide vanes.- At survey station 2 the velocity-ratio distributions with guide vanes (fig. 10) indicate that the flow at 175° improved considerably from the velocity distributions for the original vane configuration. A plot of the distribution of the flow angle β for various circumferential angles is presented in figure 11. The flow-angle measurements were selected so as to fall between the wakes of the guide vanes. The data points of figure 7 were not always obtained in this region. The data follow closely the trend of the curve predicted by the methods of references 4 and 5. At a given distance from the rotor hub, the data scatter was approximately ±3° with changes in circumferential angle. This variation approaches the accuracy of the data.

CONCLUDING REMARKS

Results of total-pressure surveys at the exit of a particular space-limited inlet-elbow installation revealed that a low-energy region existed at the inner part of the elbow because of flow separation. The simple addition of a single vane upstream of and near the inner turn eliminated the flow separation and greatly improved the velocity and total-pressure distribution in the region. The investigation also revealed, as has been shown elsewhere, that the addition of the guide vanes tends also to produce a more uniform flow distribution at the entrance to the compressor.

Langley Research Center,
National Aeronautics and Space Administration,
Langley Station, Hampton, Va., March 19, 1965.

REFERENCES

1. Wilbur, Stafford W.: An Investigation of Flow in Circular and Annular 90° Bends With a Transition in Cross Section. NACA TN 3995, 1957.

2. Henry, John R.: Design of Power-Plant Installations. Pressure-Loss Characteristics of Duct Components. NACA WR L-208, 1944. (Formerly NACA ARR L4F26.)

3. Valentine, E. Floyd; and Copp, Martin R.: Investigation To Determine Effects of Rectangular Vortex Generators on the Static-Pressure Drop Through a 90° Circular Elbow. NACA RM L53G08, 1953.

4. Emery, James C.; Herrig, L. Joseph; Erwin, John R.; and Felix, A. Richard: Systematic Two-Dimensional Cascade Tests of NACA 65-Series Compressor Blades at Low Speeds. NACA Rept. 1368, 1958. (Supersedes NACA TN 3916 by Herrig, Emory, and Erwin and NACA TN 3913 by Felix.)

5. Herrig, L. Joseph; Emery, James C.; and Erwin, John R.: Effect of Section Thickness and Trailing-Edge Radius on the Performance of NACA 65-Series Compressor Blades in Cascade at Low Speeds. NACA RM L51J16, 1951.

6. Schulze, Wallace M.; Ashby, George C., Jr.; and Erwin, John R.: Several Combination Probes for Surveying Static and Total Pressure and Flow Direction. NACA TN 2830, 1952.

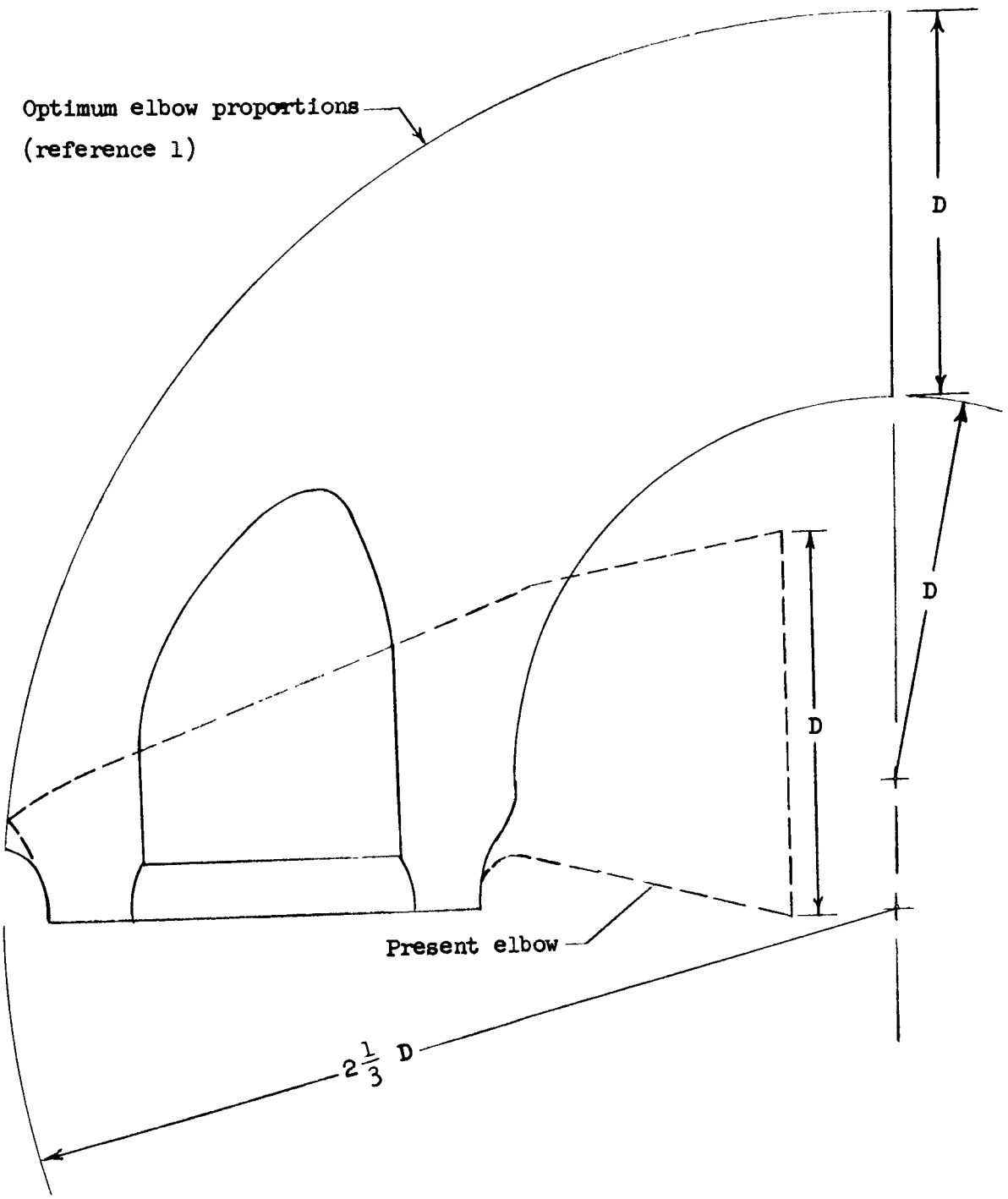

Figure 1.- Optimum elbow proportions as compared with the elbow of the present investigation.

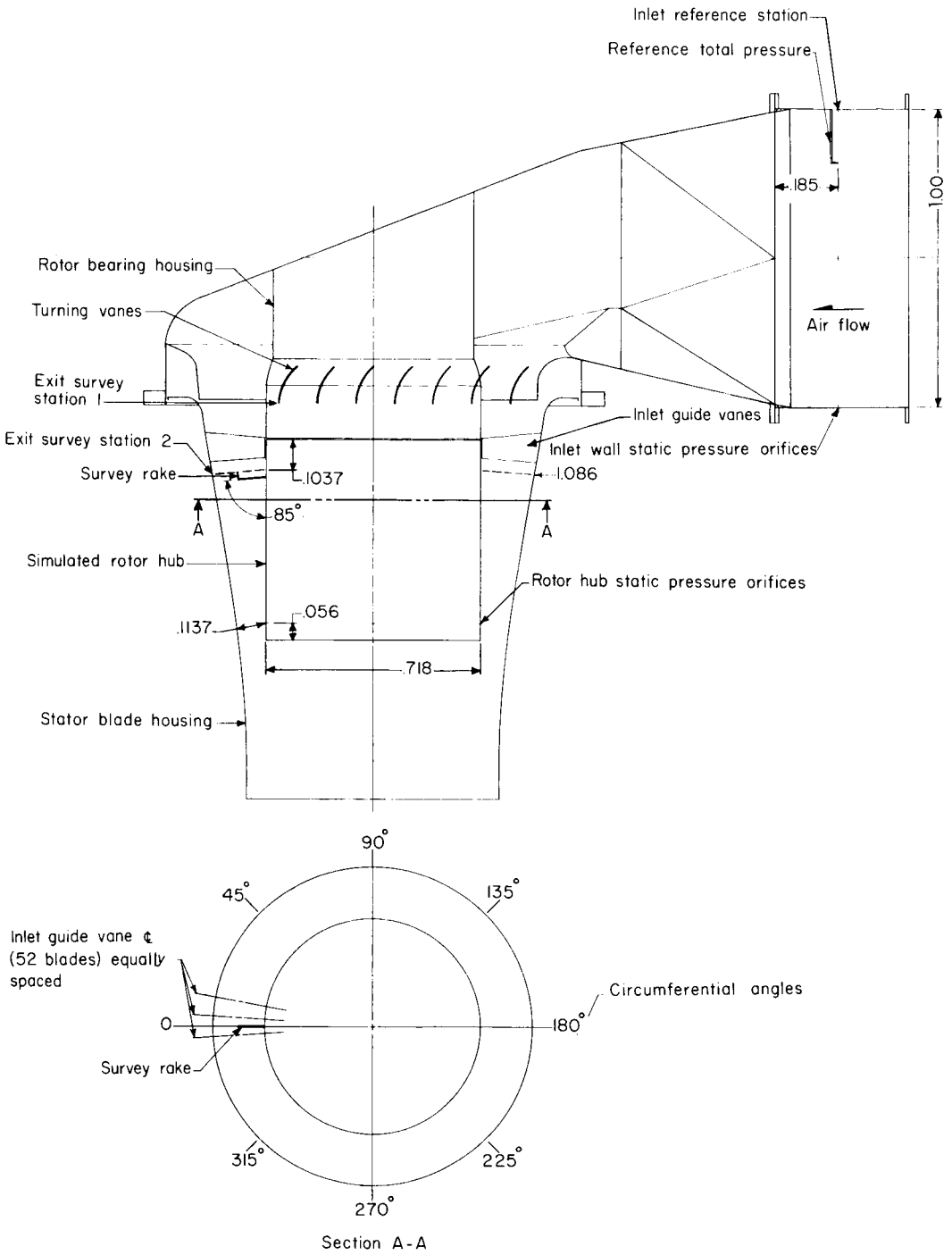

(a) Original vane configuration.

Figure 2.- General arrangement of apparatus and vane configuration. All dimensions are in terms of inlet diameter.

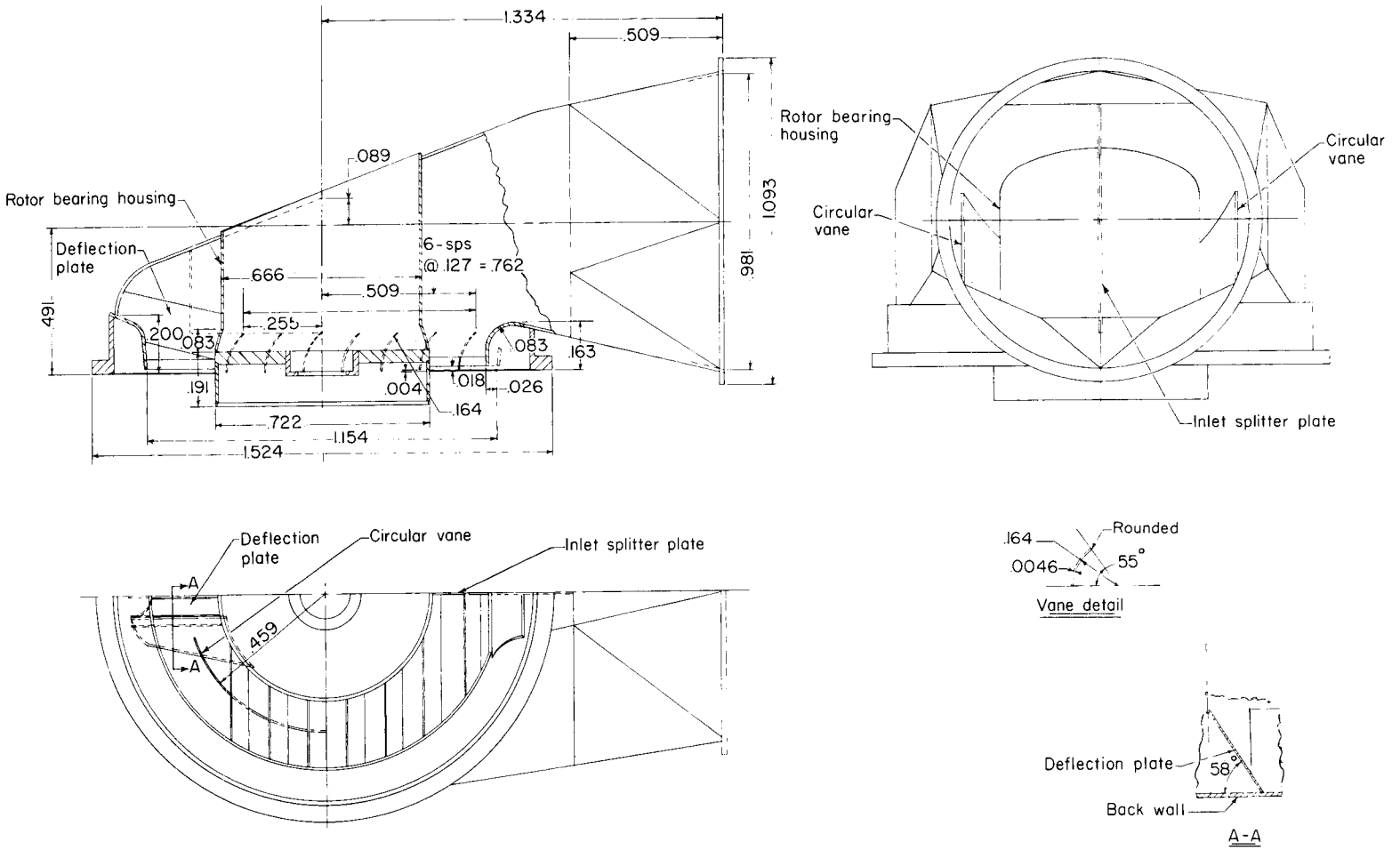

(b) Schematic of inlet elbow.

Figure 2.- Continued.

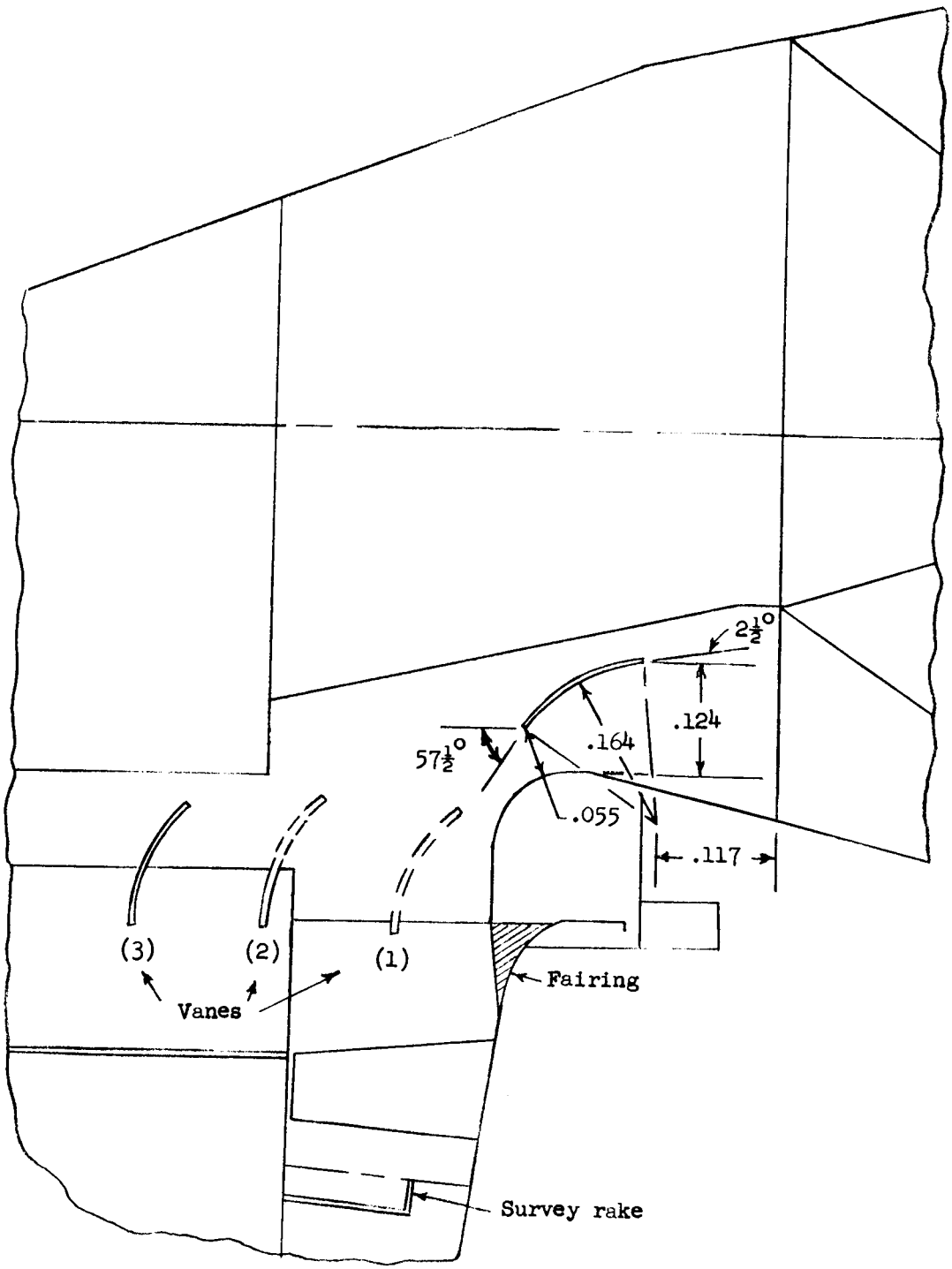

(c) Final vane modification. Note: Vane 1 and the leading 16.1° of vane 2 were removed (indicated by dotted lines).

Figure 2.- Continued.

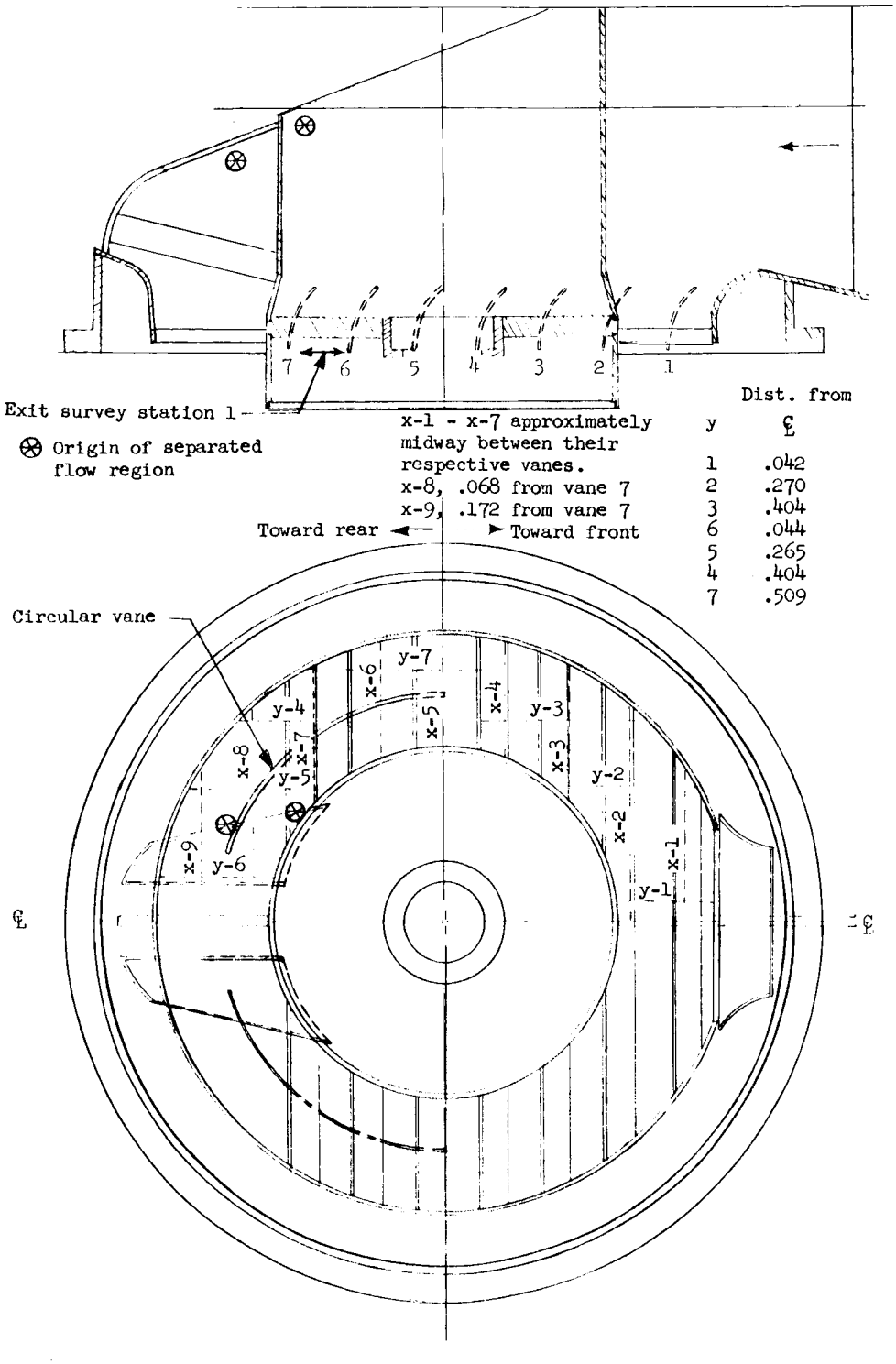

(d) General survey arrangement of elbow without stator-blade housing.

Figure 2.- Concluded.

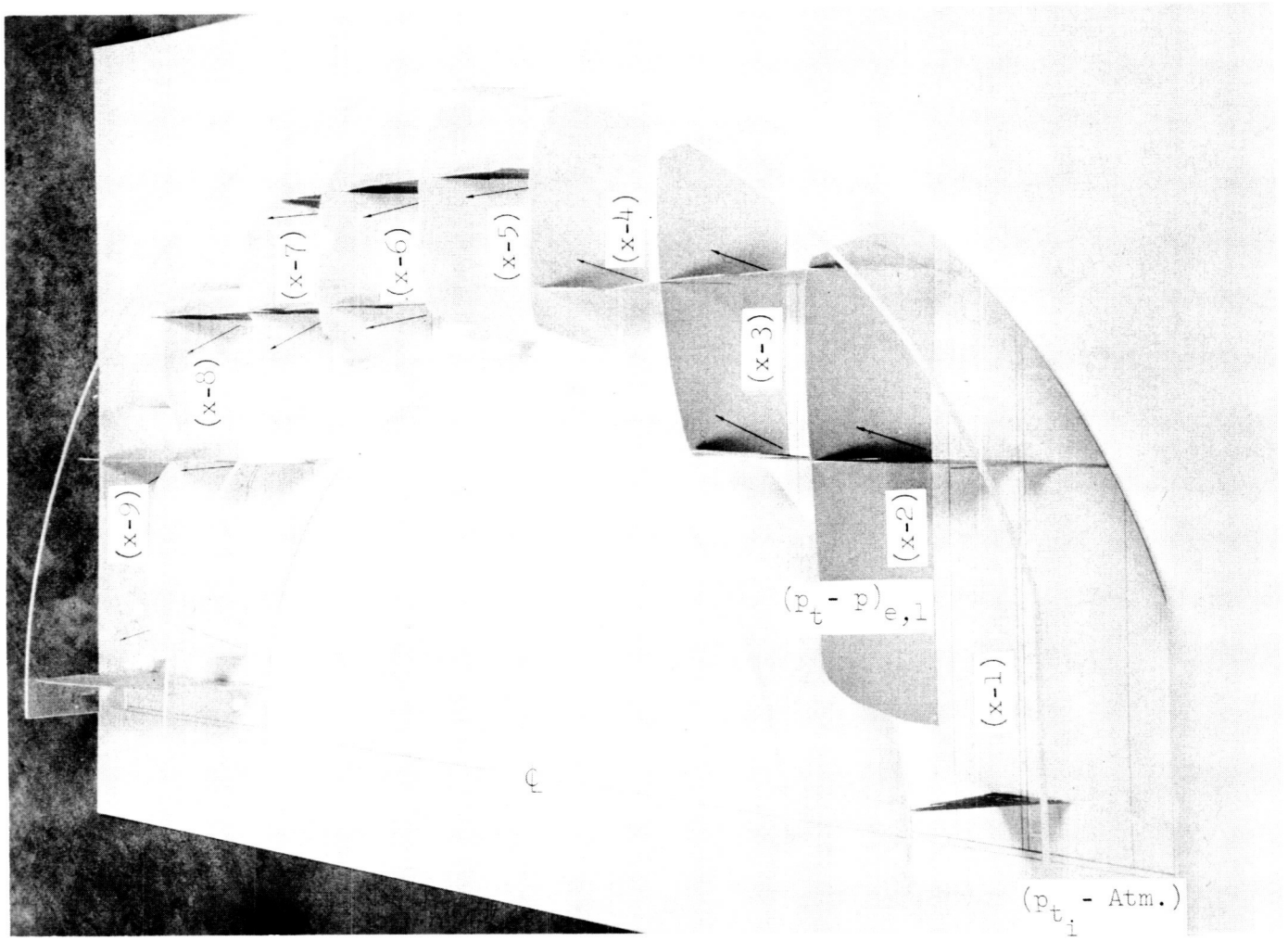

(a) View A.

L-65-66

Figure 3.- Total pressure contours and flow direction of elbow without a downstream section of ducting.

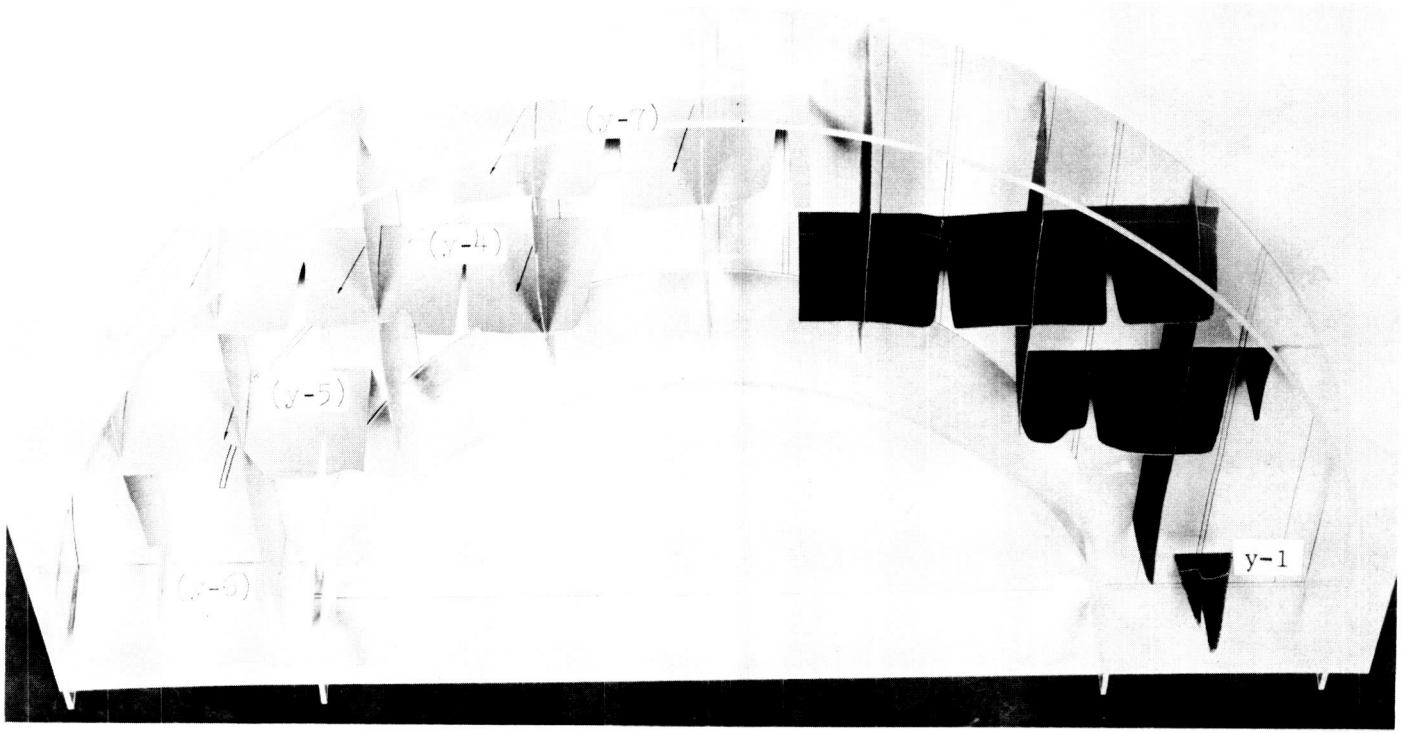

(b) View B. L-65-67

Figure 3.- Continued.

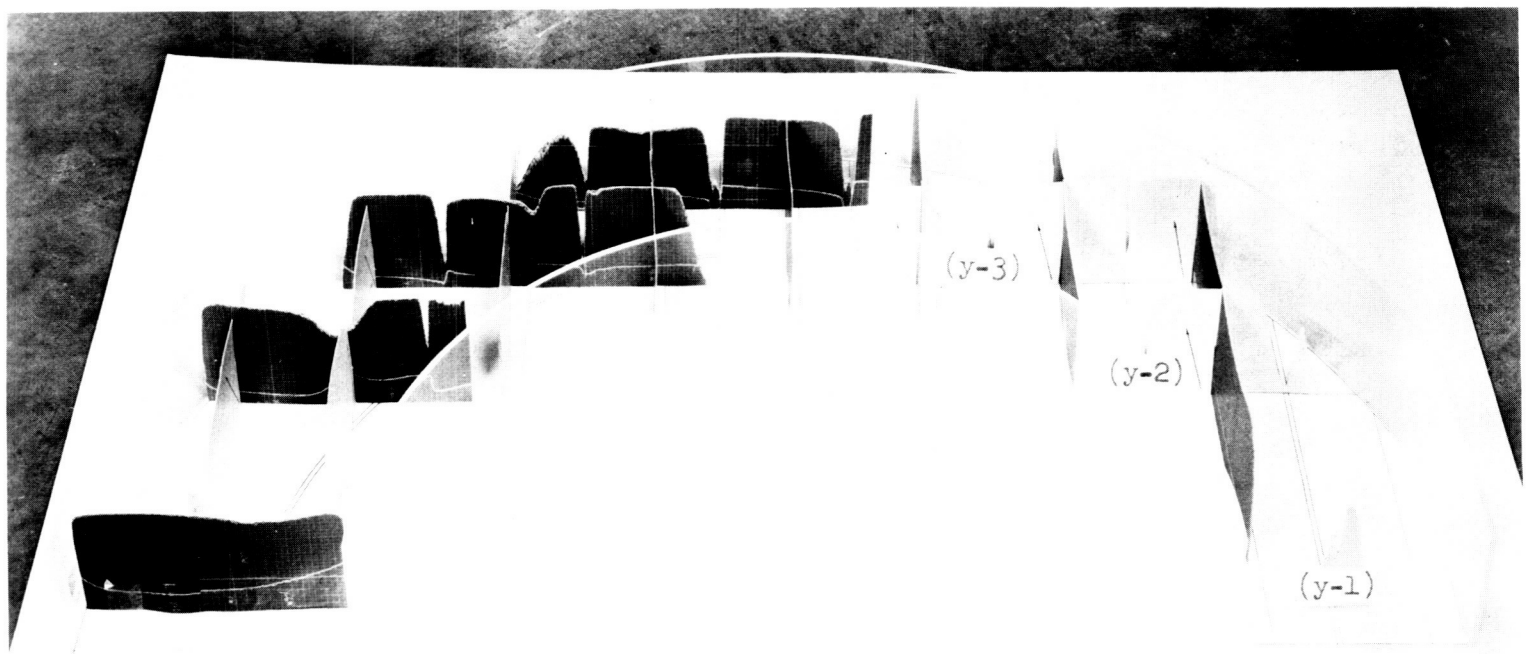

(c) View C. L-65-68

Figure 3.- Continued.

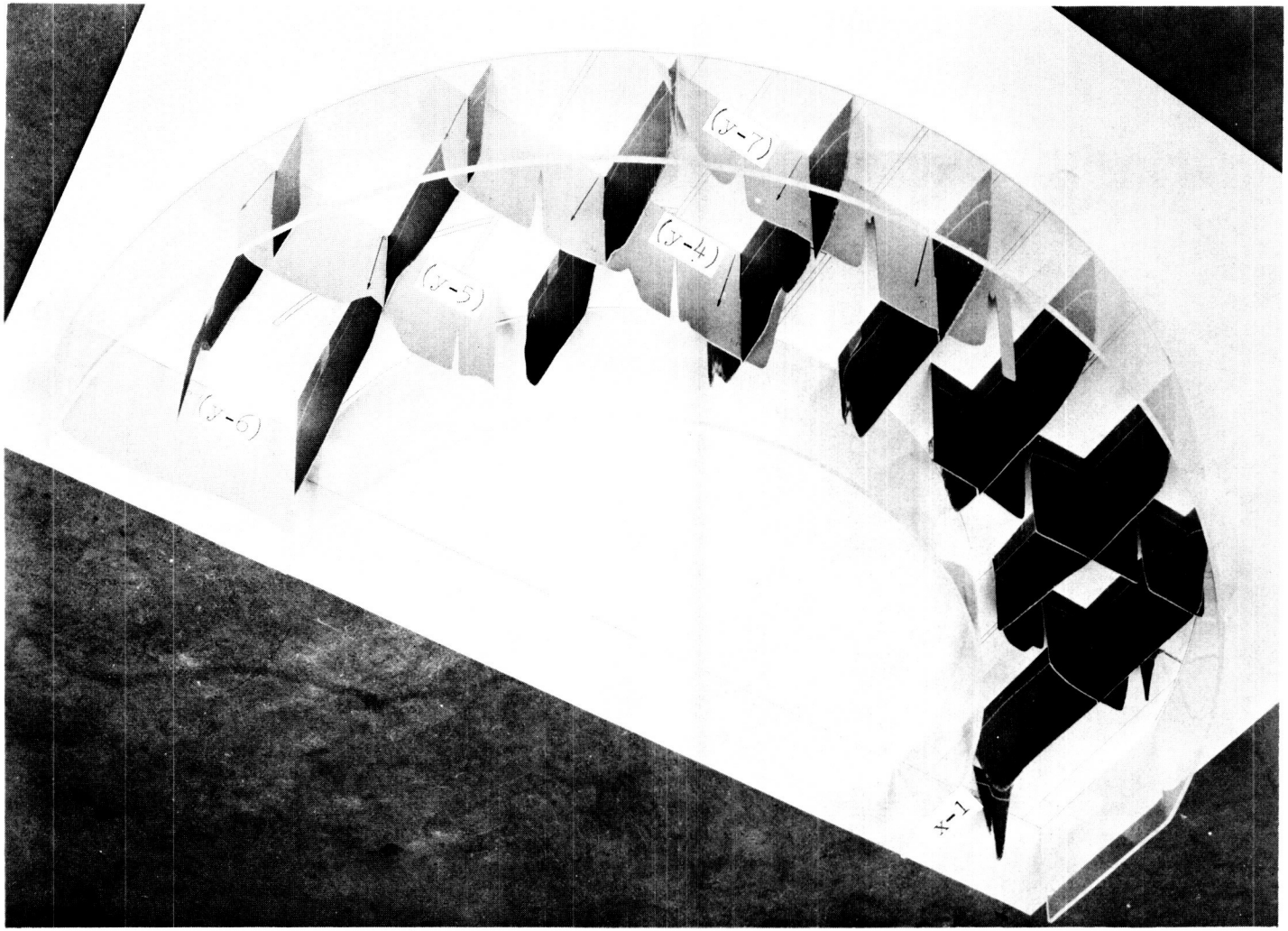

(d) View D. L-65-69

Figure 3.- Continued.

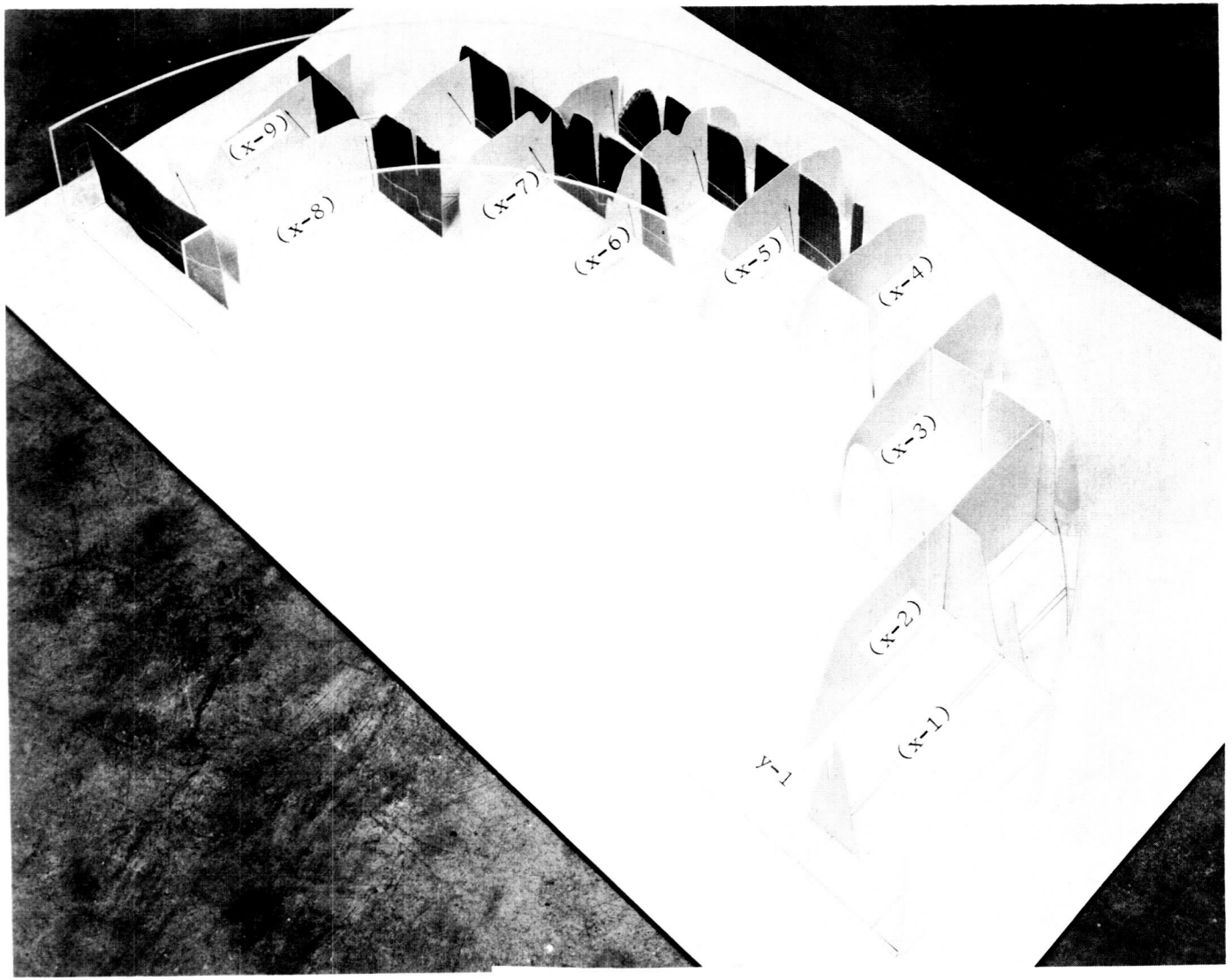

(e) View E.

L-65-70

Figure 3.- Concluded.

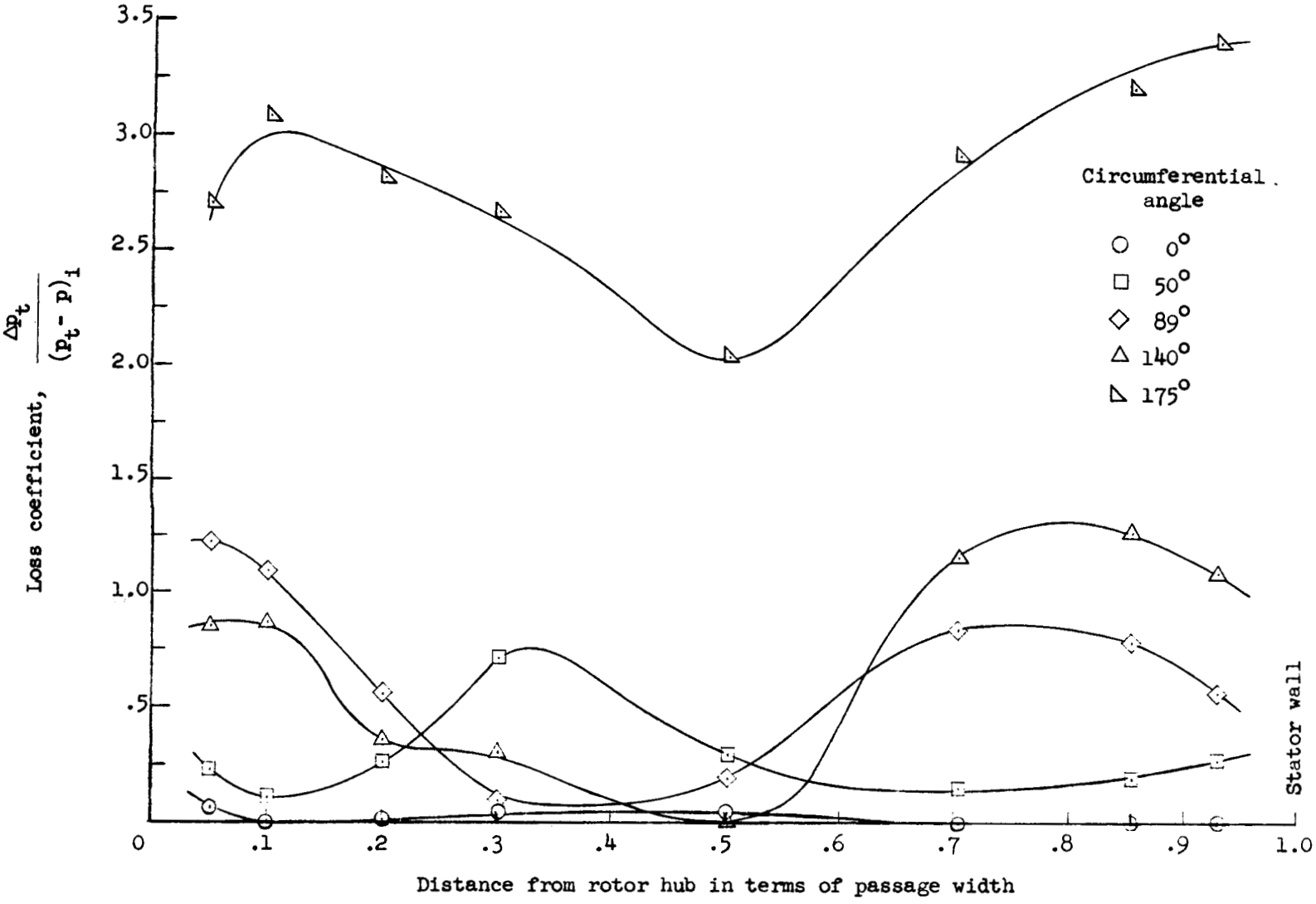

Figure 4.- Local radial variation of loss coefficient for elbow with a stator-blade housing and without guide vanes but with the original vane configuration.

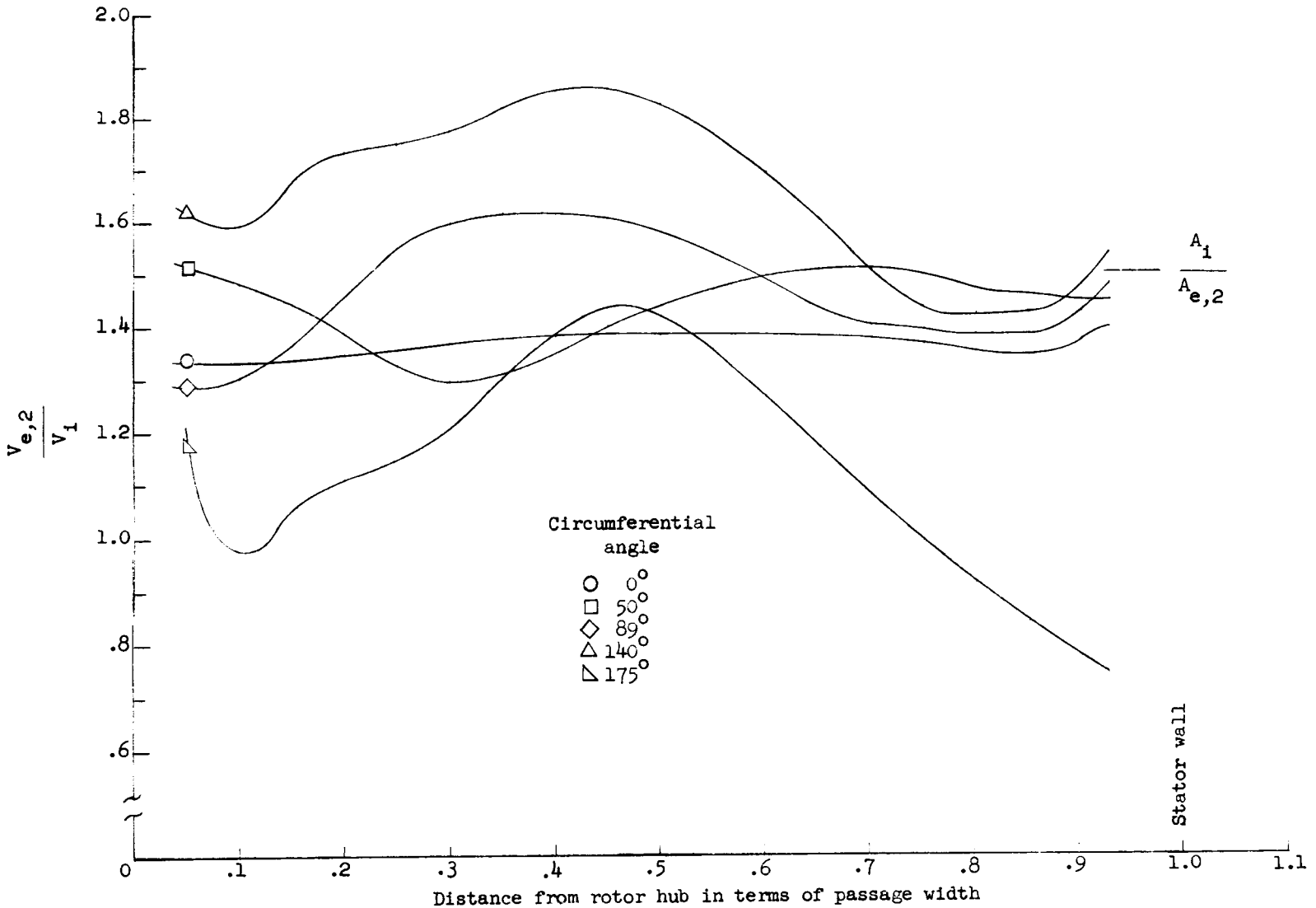

Figure 5.- Radial variations of velocity for elbow with a stator-blade housing and without guide vanes but with the original vane configuration.

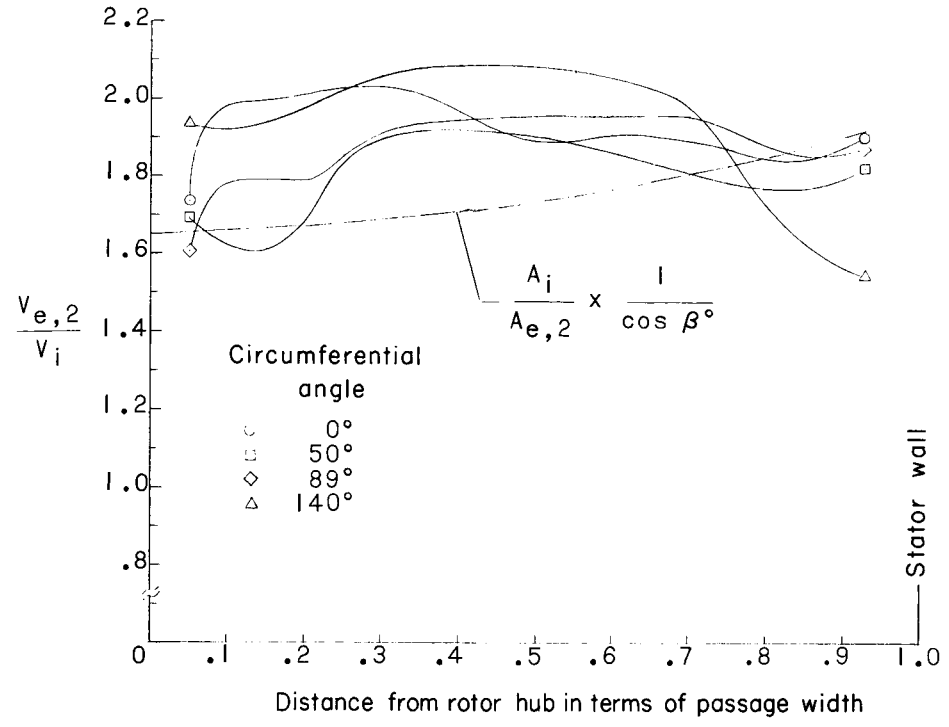

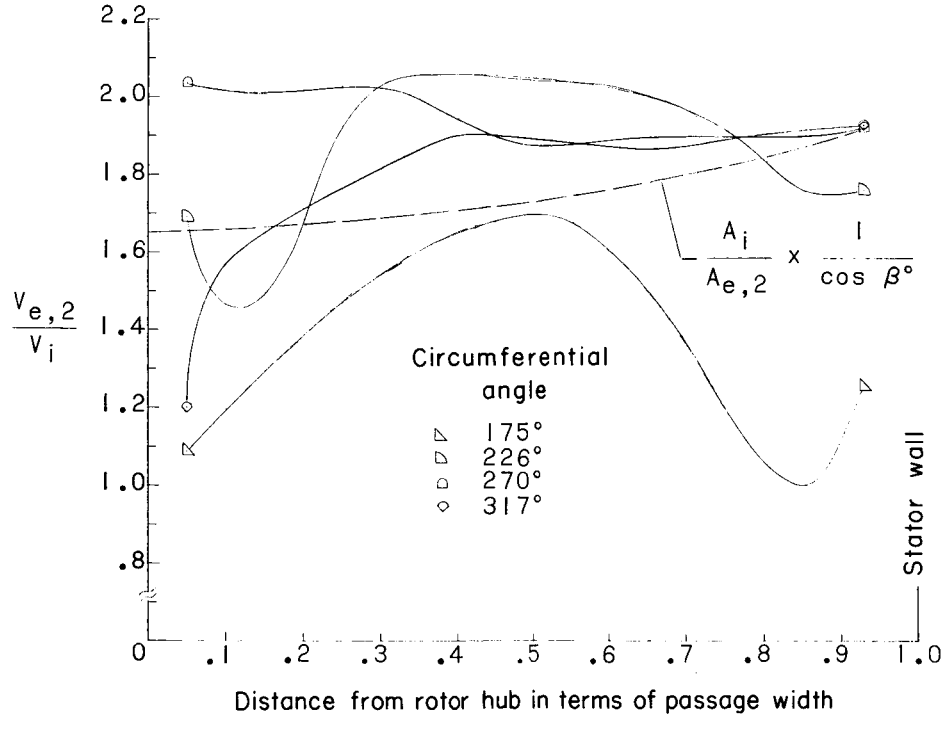

Figure 6.- Radial variation of velocity for elbow with a stator-blade housing and guide vanes, but with the original vane configuration.

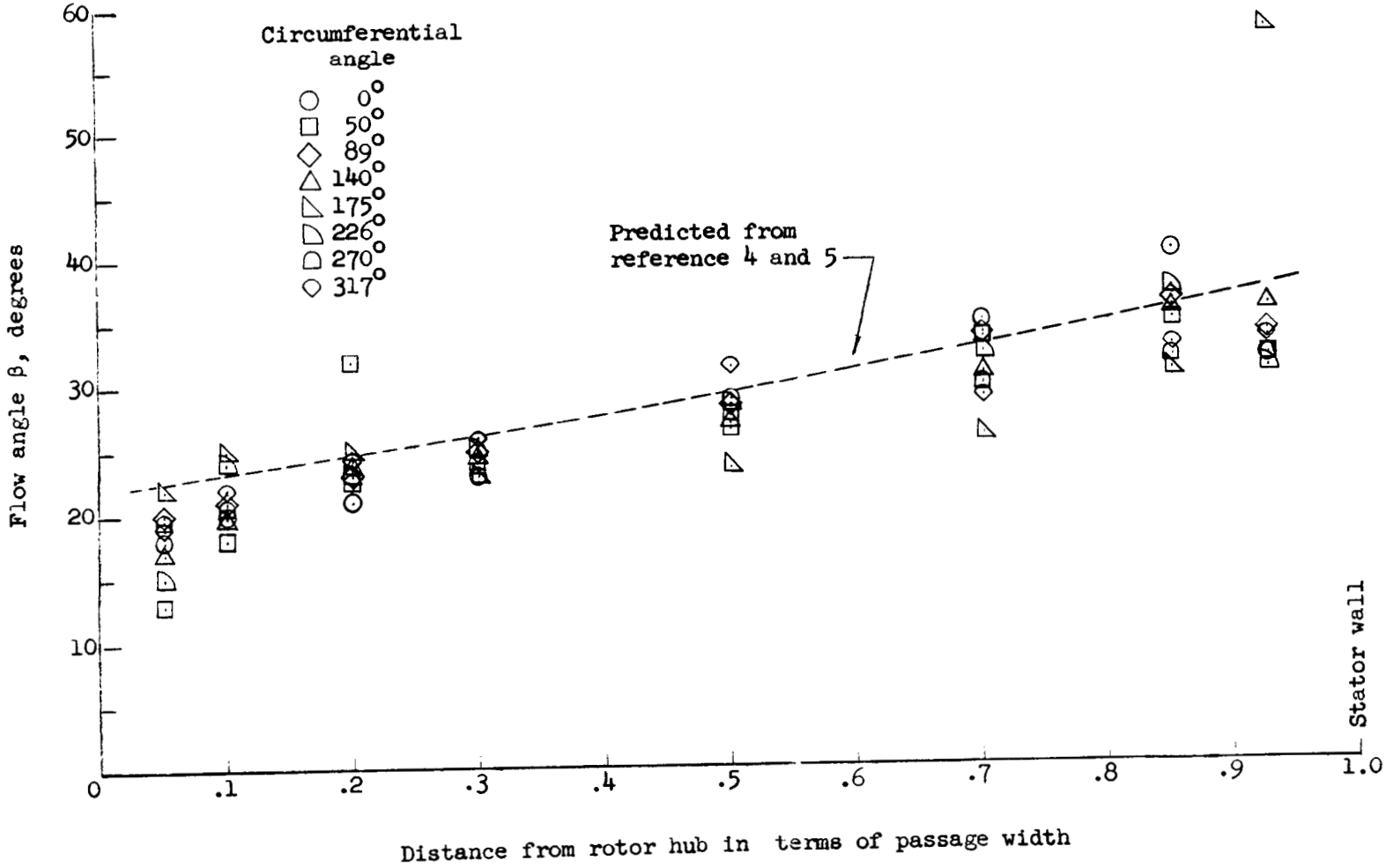

Figure 7.- Radial variations of flow angle for elbow with a stator-blade housing and guide vanes but with the original vane configuration.

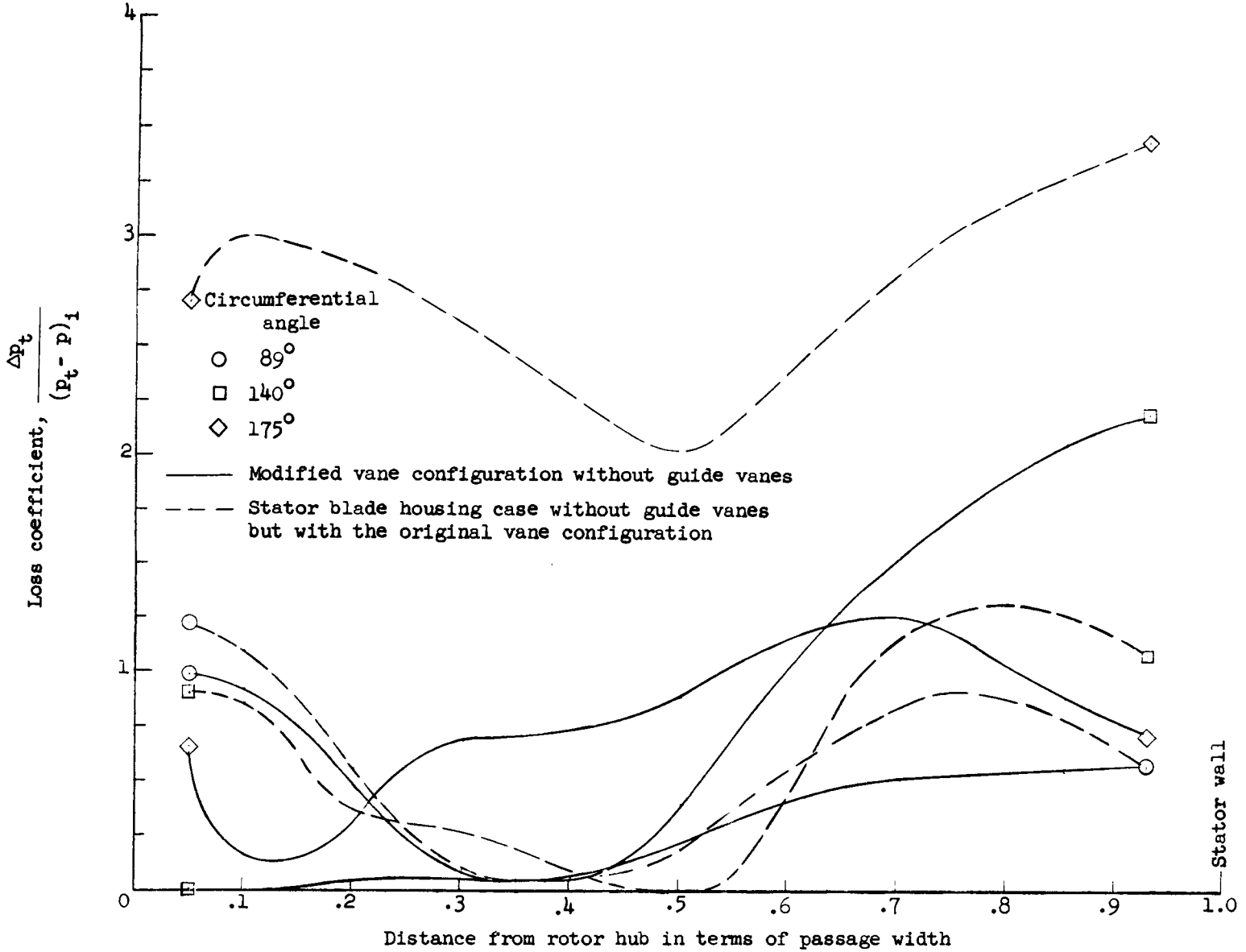

Figure 8.- Local radial variation of loss coefficient with a stator-blade housing, rotor hub, and modified vane configuration but without guide vanes.

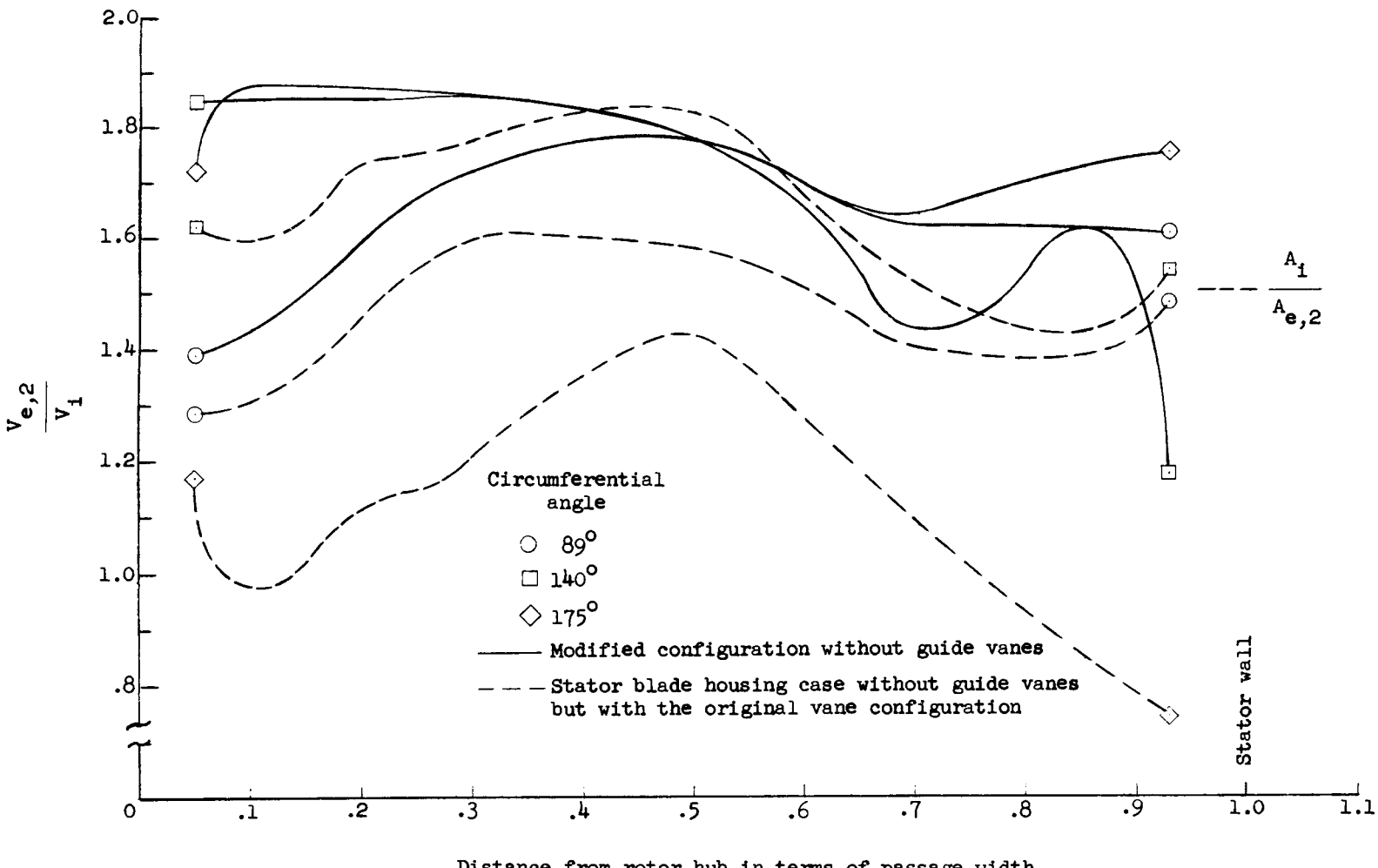

Figure 9.- Radial variation of velocity with a stator-blade housing, simulated rotor hub, and modified vane configuration but without guide vanes.

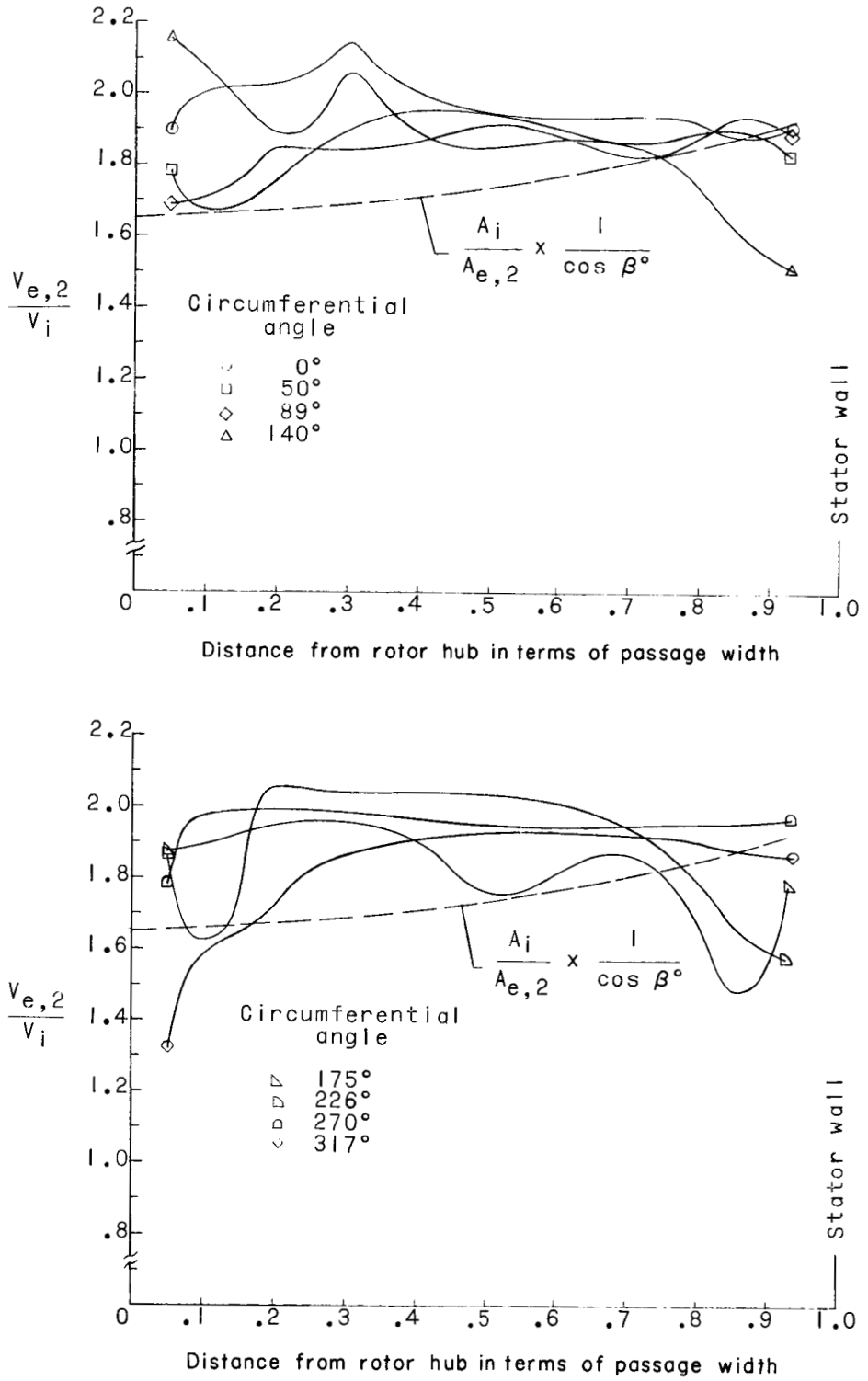

Figure 10.- Radial variation of velocity with a stator-blade housing, rotor hub, modified vane configuration, and guide vanes.

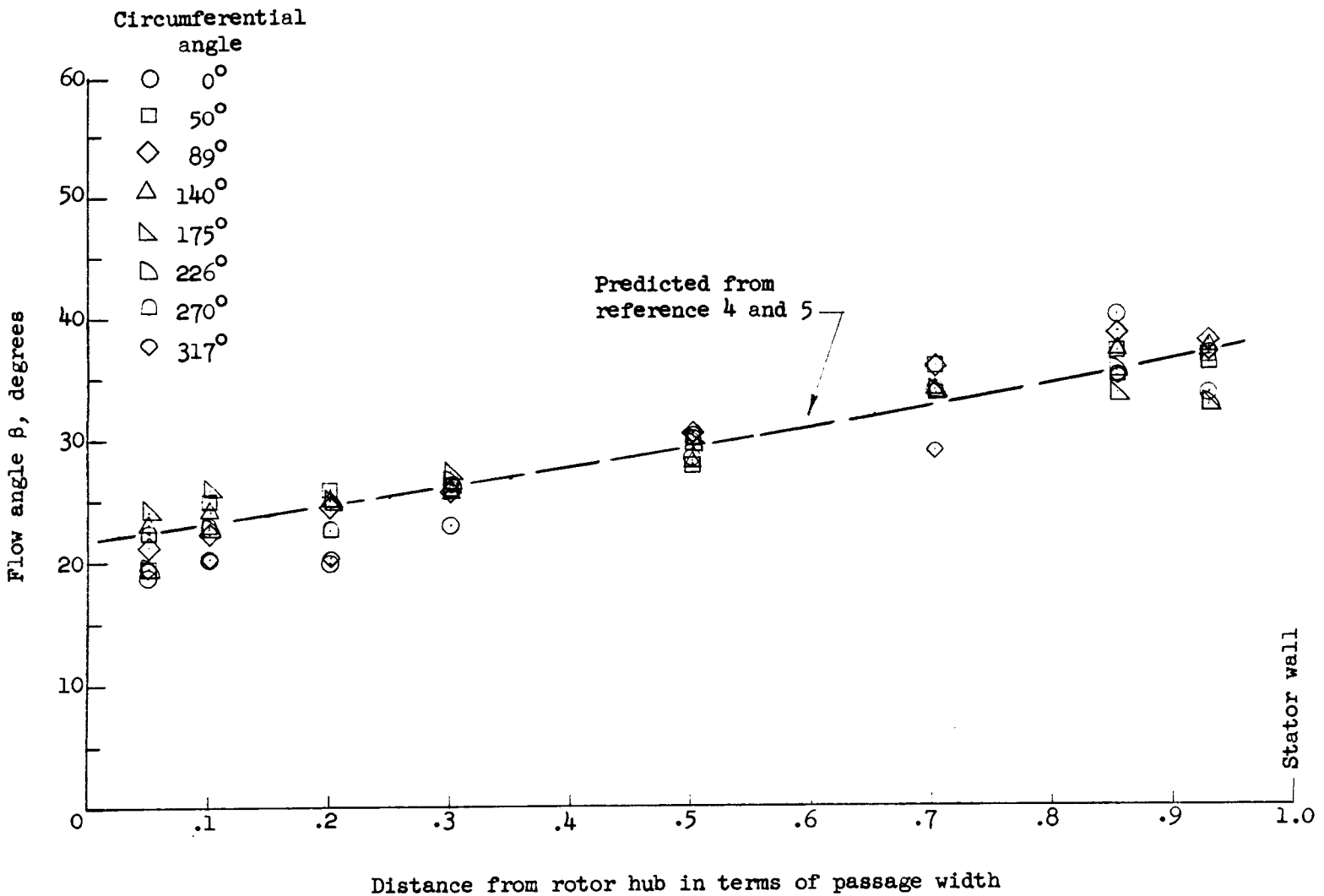

Figure 11.- Radial variation of flow angle with stator-blade housing, rotor hub, modified vane configuration, and guide vanes.